Heliyon 10 (2024) e24408

Contents lists available at ScienceDirect

Heliyon

journal homepage: www.cell.com/heliyon

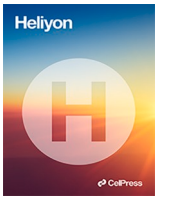

Research article

NUPR1 contributes to activate TFE3-dependent autophagy leading to cervical cancer proliferation

Xiaoguang Wang [a,1], Ke Wang [b,1], Xiuli Wang [c,*]

[a] Department of Gynaecology, Yantaishan Hospital, Yantai, Shandong, China
[b] Department of Gynaecology, Yeda Hospital, Yantai, Shandong, China
[c] Department of Gynecology, The Affiliated Yantai Yuhuangding Hospital of Qingdao University, Yantai, Shandong, China

ARTICLE INFO

Keywords:
Cell apoptosis
Autophagy
PI3K/Akt signaling
Xenograft tumor

ABSTRACT

Cervical cancer is a malignant tumor that occurs in the cervix of women and endangers their lives. In this study, we aimed to assess the roles of NUPR1 and TFE3 in cervical cancer. The Cancer Genome Atlas (TCGA) database was used to assess the correlation between NUPR1 and TFE3 expression in cervical cancer. By silencing NUPR1 and TFE3, and through 3-MA treatment, we determined whether their silencing could lead to lysosomal dysfunction, thereby inhibiting autophagy and cervical cancer cell proliferation. Their roles were further analyzed using molecular biological methods. Silencing NUPR1 and TFE3 inhibited cell proliferation and decreased the expression levels of autophagy-related genes, p62 and LC3B. By tracing lysosomes within cells, NUPR1 and TFE3 knockdown were found to induce lysosomal dysfunction, thereby inhibiting autophagy. *In vivo* experimental studies have shown that knockdown of NUPR1 and TFE3 can inhibit tumor growth, while reducing the ki67, p62, and LC3B expression levels and promoting apoptosis. Furthermore, the expression levels of lamp1 and lamp2, and the phosphorylation of PI3K (p-PI3K) and Akt (p-Akt) were significantly reduced after NUPR1 and TFE3 knockdown. However, treatment with 3-MA and overexpression of TFE3 could partially reverse the effect of silencing NUPR1. Overall, silencing NUPR1 reduced autophagy by inhibiting TFE3 in cervical cancer. Our results supply new evidence for the use of NUPR1 as a therapeutic target in cervical cancer.

1. Introduction

Cervical cancer is the second most common malignancy in women worldwide with approximately 570,000 new cases and 311,000 deaths every year, worldwide. The incidence and mortality of cervical cancer in low- and middle-income countries are second only to breast cancer [1]. China has approximately 130,000 new cervical cancer cases annually, accounting for 28 % of the total cervical cancer cases globally [2]. Currently, surgery, radiotherapy, and chemotherapy are the main treatment strategies for cervical cancer [3]. Therefore, further exploration of the mechanisms involved in cervical cancer and the search for potential molecular targets for predicting its occurrence and progression have important clinical value in improving the prognosis and survival of patients with

* Corresponding author. Department of Gynecology, the Affiliated Yantai Yuhuangding Hospital of Qingdao University, No 20 Yuhuangding East Road, Yantai, 264000, Shandong, China.
E-mail address: wamtai81702@sina.com (X. Wang).
[1] These authors contributed equally to the current study.

https://doi.org/10.1016/j.heliyon.2024.e24408
Received 21 August 2023; Received in revised form 1 December 2023; Accepted 8 January 2024
Available online 12 January 2024

cervical cancer.

Nuclear protein transcription regulator 1 (NUPR1), a small molecular stress nuclear protein expressed in acute pancreatitis, exists as an intrinsically disordered protein with 82 residues. NUPR1 participates in various pathophysiological processes, such as pancreatic injury, liver injury, diabetes, breast cancer, liver cancer, and renal cancer [4–9]. NUPR1 is expressed in most tumor tissues and participates in the cancer cell cycle, apoptosis, drug sensitivity, invasion, and metastasis. Further, NUPR1 can affect the resistance of cancer cells to anticancer drugs [10]. NUPR1 is known to inhibit pancreatic cancer growth [4]. A recent study showed that NUPR1 can regulate autophagy-induced apoptosis in multiple myeloma cells through the photoshatidylinositol 3 kinase (PI3K)/protein kinase B (Akt) pathway [11]. Real et al. analyzed the changes in NUPR1 expression in tissue biopsies tissues from 14 patients with cervical cancer before and after cisplatin adjuvant chemotherapy and found a downward trend in NUPR1 expression [12]. However, the role of NUPR1 in cervical cancer remains unclear.

Microphthalmia family of bHLH-LZ transcription factor TFE3 (transcription factor binding to IGHM enhancer 3) is a transcriptional regulator of autophagy and lysosomal biogenesis [13]. There are homologs and heterodimers of TFEB and TFE3, they can bind to each to promote and activate several genes [14–16]. Their function is redundant in some cellular environments, but essential in others [14, 17,18]. Recent studies have shown that NUPR1 promotes cell proliferation and metastasis both in oral squamous cell carcinoma and breast cancerby activating TFE3-dependent autophagy [4,13]. However, whether NUPR1 affects cervical cancer cell proliferation by activating TFE3-induced autophagy remains to be studied.

We investigated the relationship between NUPR1 and TFE3 expression in cervical cancer in the present study. We determined whether silencing NUPR1 and TFE3 leads to lysosomal dysfunction, thereby inhibiting autophagy and cell proliferation, to explore the underlying mechanism. This study will help elucidate the mechanism of NUPR1 involvement in cervical cancer and develop new targets for cervical cancer diagnosis and treatment.

2. Material and methods

2.1. Analysis of The Cancer Genome Atlas (TCGA)

TCGA (https://portal.gdc.com) provided NUPR1 and TFE3 RNA-sequencing expression profiles (level 3) and the associated clinical information. With the help of the R software package ggstatsplot, two-gene correlation maps were visualized and a multi-gene correlation heatmap was generated. With a log-rank test, survival differences between groups were compared. Time ROC analysis (v 0.4) was used to compare the predictive accuracy of NUPR1 and TFE3 mRNA levels.

2.2. Cell culture

HeLa and SiHa cells (Type Culture Collection of the Chinese Academy of Sciences, Shanghai, China) were grown in RPMI 1640 medium (Gibco, USA) containing 10 % fetal bovine serum (FBS; Gibco, USA) and Dulbecco's modified Eagle's medium (DMEM; Gibco, USA) supplemented with 10 % FBS, respectively. The cells were cultured in an incubator (ThermoFisher Scientific, USA) containing 5 % CO_2 at 37 °C. 3-Methyladenine (3-MA, an autophagy inhibitor) and recombined human TFE3 (rhTFE3) were obtained from Abcam (Cambridge, MA, USA).

2.3. Transfection

Cells were grown in 6-well plates. Negative control shRNAs for NUPR1 (NC1) and TFE3 (NC2), shNUPR1, and shTFE3 (100 nmol/L, Genechem, Shanghai, China) were transfected into the cells using Lipofectamine® 3000 kits (Invitrogen, USA), and then used for further experiments after 48 h of incubation.

2.4. RT-qPCR

TRIzol reagent (Takara, Japan) was utilized to extract total RNA from cells or tissues. cDNA synthesis and analysis were performed using a PrimeScript RT kit (Takara, Japan). PCR process was performed using SYBR Premix Ex Taq (Takara, Japan). Endogenous GAPDH was adopted as a control. The relative mRNA expression levels of NUPR1 and TFE3 were determined using the $2^{-\Delta\Delta Ct}$ method.

2.5. Wound healing assay

Cells were cultivated in a 12-well culture dish (5×10^4 cells in each well) and incubated at 37 °C in medium without FBS. After the cells achieved 80 % confluency, a 10 μL pipette tip was utilized to scratch on the dish surface. The scratches were observed after 24 h of incubation with different treatments.

2.6. Transwell assay

Different transfected cells (2.5×10^4) were cultured in the Matrigel-coated upper chamber. The cells were allowed to invade the bottom chamber filled with 10 % FBS-containing culture medium, after incubation at 37 °C for 24 h. Invading cells were fixed in methanol and stained at room temperature with 0.1 % crystal violet, then photographed for each sample utilizing an optical

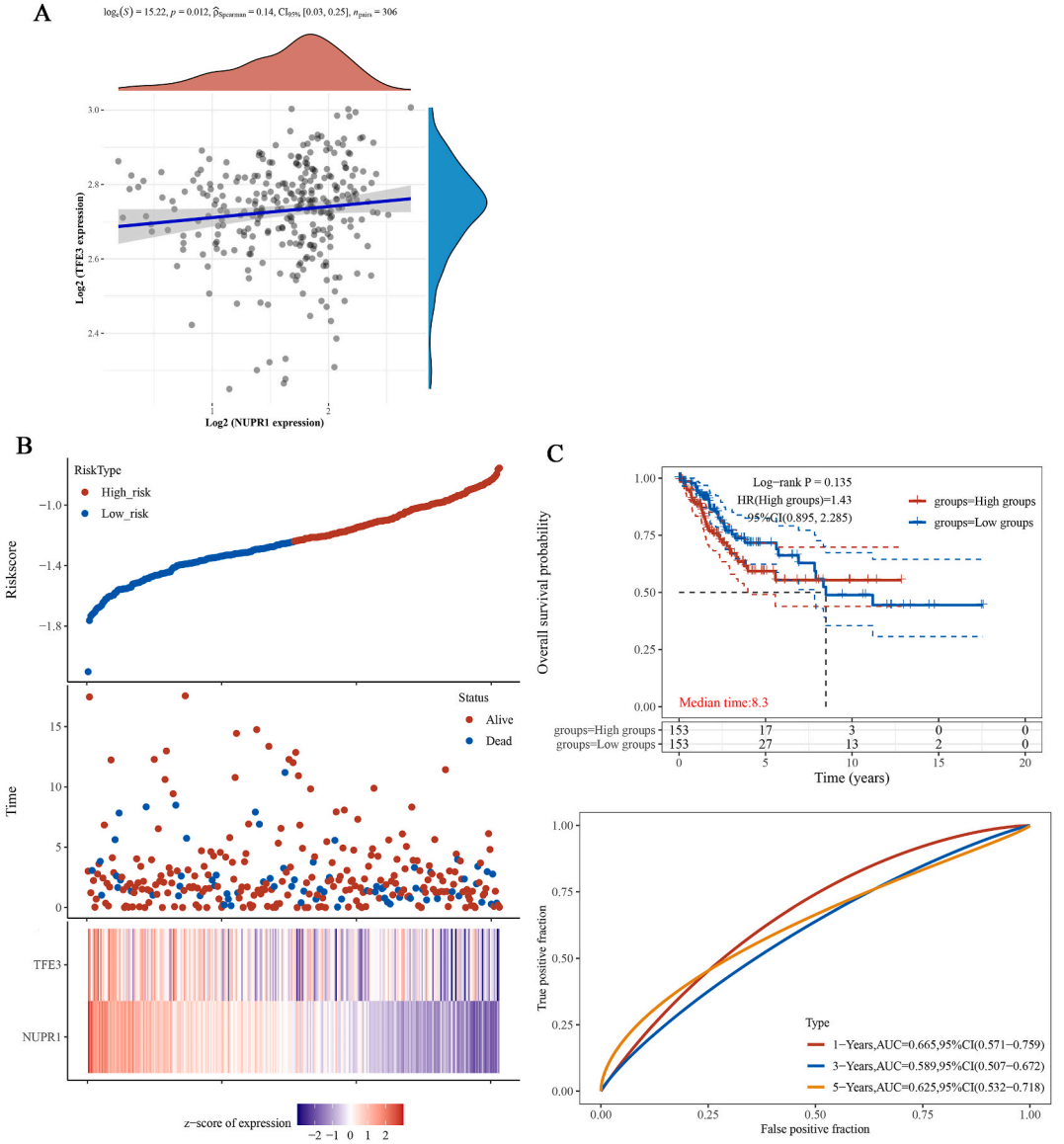

Fig. 1. Online analysis of NUPR1 and TFE3 expression in cervical cancer using TCGA database. A: TCGA database was analyzed for the correlation between NUPR1 and TFE3 expression levels in cervical cancer tissue; B: The expression time and risk coefficient of NUPR1 and TFE3 in cervical cancer tissue; C: The impact of NUPR1 and TFE3 on the survival rate of patients with cervical cancer.

microscope (magnification, × 100).

2.7. Clone formation assay

The cells were cultivated in 6-well plates with 500 cells per well. After 2 weeks of treatment using different methods, a total of 100 % methanol was used to fix the cells followed by 0.5 % crystal violet for staining. Images were then captured and the number of colonies was counted.

2.8. EdU assay

Logarithmic growth-stage cells were collected for routine digestion, centrifugation, and resuspension. The cells were incubated in a 96-well plate at a density of 4×10^3 cells per well. The cells were treated according to different groups following the instructions of the reagent kit (Thermo Fisher Scientific, USA) to perform EdU staining. A fluorescence microscope (Leica, Germany) was used to obtain images.

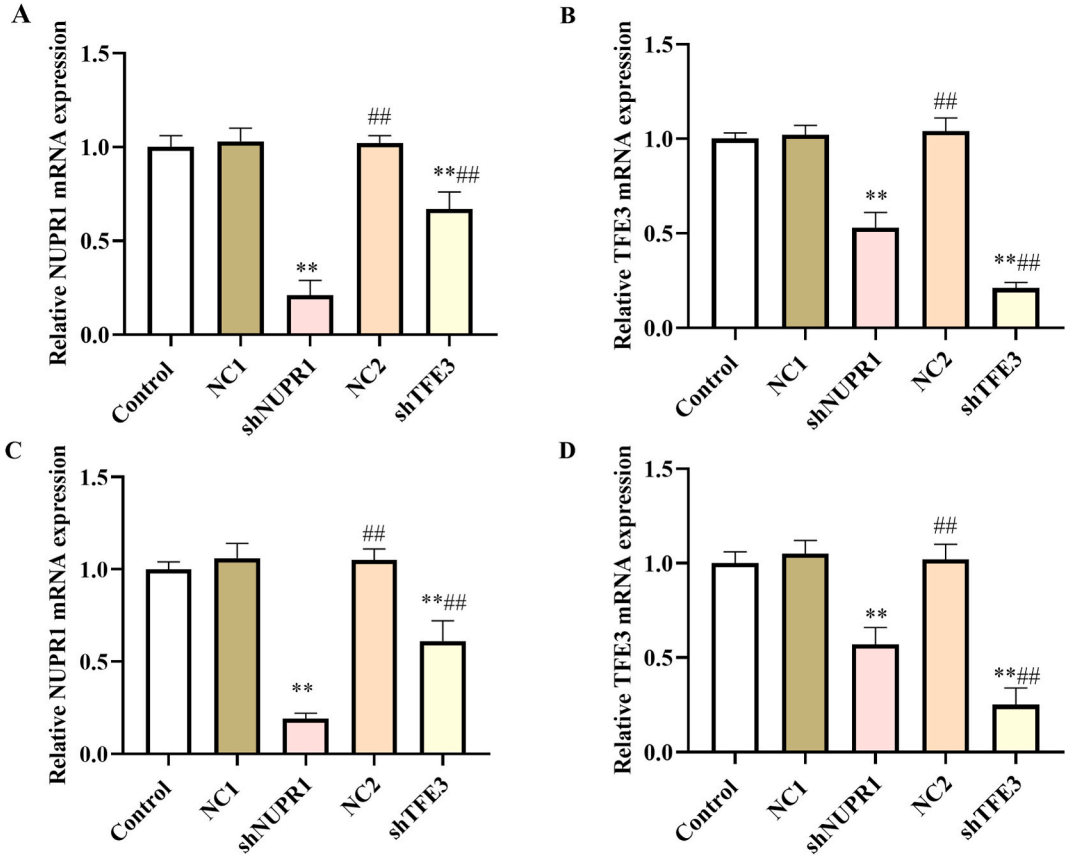

Fig. 2. NUPR1 or TFE3 knockdown can significantly decrease the expression of NUPR1 or TFE3. The relative mRNA expression of NUPR1 (A) and TFE3 (B) in HeLa cells using qRT-PCR; The relative mRNA expression of NUPR1 (C) and TFE3 (D) in SiHa cells using qRT-PCR. NC1 means negative control shRNA for NUPR1, NC2 means negative control shRNA for TFE3. n = 3. versus control group or NC group, *P < 0.05, **P < 0.01; versus shNUPR1 group, $^{\#}$P < 0.05, $^{\#\#}$P < 0.01.

2.9. Immunofluorescence

After different treatments, the cells were washed with PBS, and 3.7 % formaldehyde was applied for 30 min. After two washes with PBS, the cells were permeabilized with 0.3 % Triton X-100 in PBS for 10 min at room temperature, then the cells were incubated 5 % BSA for 1 h. Primary antibodies against NUPR1 (orb101189, Biorbyt, UK), TFE3 (orb214656, Biorbyt, UK), p62 (orb12443, Biorbyt, UK), and LC3B (Cell Signaling Technology, USA) were utilized to incubated with the cells at 37 °C for 2 h. The cells were washed thrice with PBS, then incubated with Alexa Fluor 488-conjugated secondary antibodies at 37 °C for 30 min and then with DAPI (2 μg/ml, Thermo Fisher Scientific, USA). Under a fluorescence microscope (Leica, Germany), cells were monitored after washed with PBS.

2.10. LysoSensor green DND-189 staining

Lysosomal staining was performed using LysoSensor Green DND-189 staining reagent (Thermo Fisher Scientific). A final concentration of 5 mM lysoSensor Green was added to the medium and incubated for 2 h at 37 °C with 5 % CO_2. A fluorescence microscope was used to visualize cells after cultivation.

2.11. Animal model

BALB/c nude mice (approximately 20 g, 6–8 weeks, Jinan Pengyue Experimental Animal Co., Ltd, Jinan, China) were placed under specific pathogen-free conditions, at 20 °C, 20 % humidity, on a 12 h light/12 h dark cycle, with free access to food and drinking water. Transfected HeLa cells were utilized to conduct the xenograft tumors. The mice were randomly divided into six groups (six mice/group): control, NC (injected with 5×10^6 sh-NC cells), sh-NUPR1 (injected with 5×10^6 sh-NUPR1 cells), sh-TFE3 (injected with 5×10^6 sh-TFE3 cells), and sh-NUPR1 + rhTFE3 (injected with 5×10^6 sh- NUPR1 cells, and intratumorally with recombined TFE3). The tumor volume was recorded and calculated as follows: V (mm^3) = length (mm) × width^2 (mm^2). After five weeks, 1 % pentobarbital sodium (400 mg/kg) was utilized by intraperitoneal injection to anesthetize the mice, and the mice were euthanized by cervical

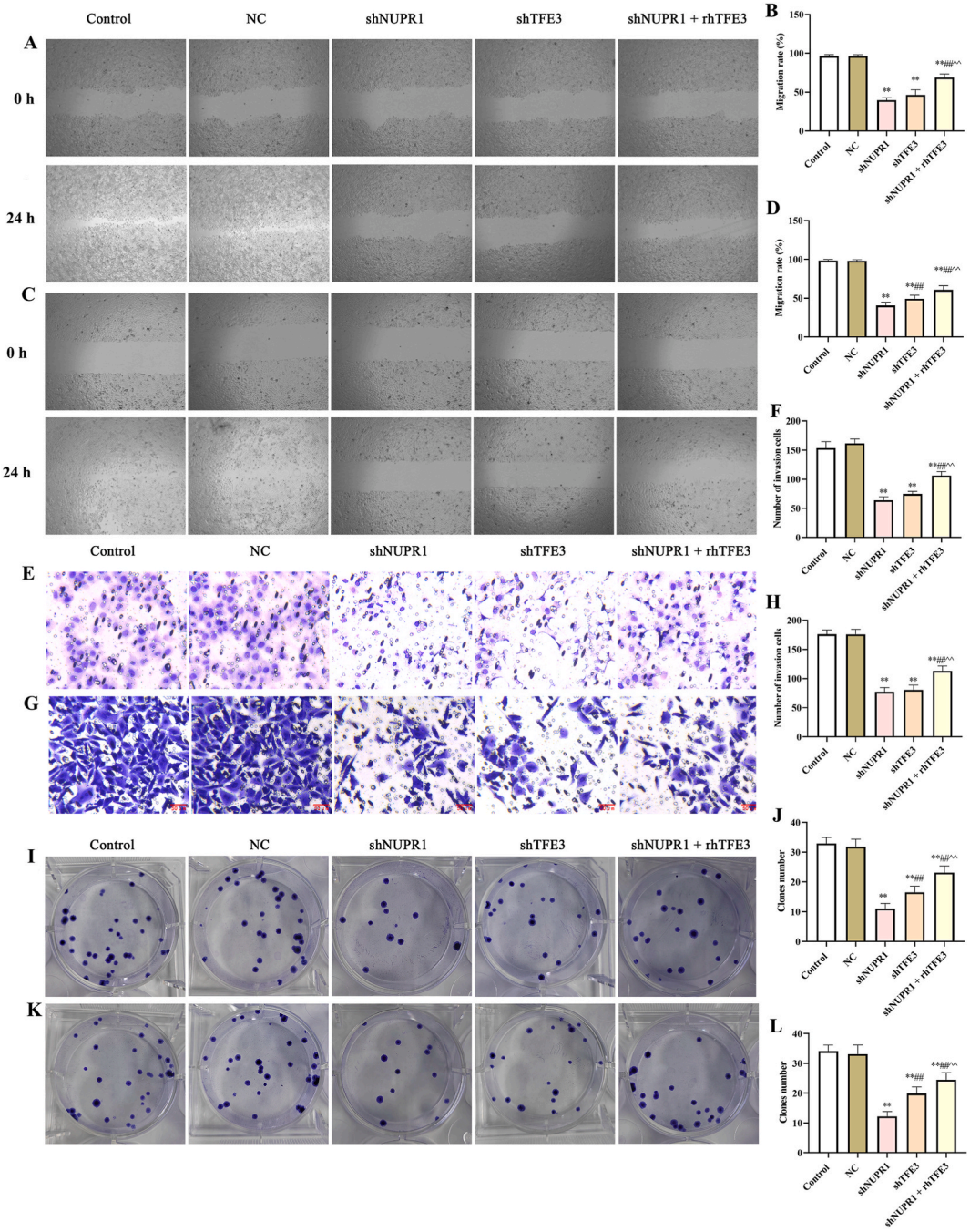

Fig. 3. NUPR1 or TFE3 knockdown can inhibit the migration, invasion, and proliferation of cervical cancer cells. Cells were divided into five groups, Control, NC (transfected with negative control shRNAs for NUPR1), shNUPR1, shTFE3, shNUPR1+rhTFE3. The migration ability of HeLa (A) and SiHa (C) cells was determined using the scratch test; Bar graph presents the quantification of migration of HeLa (B) and SiHa cells (D); Transwell detection of HeLa (E) and SiHa (G) cell invasion ability; Bar graph presenting the quantification of invasion of HeLa (F) and SiHa cells (H); Clone formation experiment to detect HeLa (I) and SiHa (K) cell proliferation ability; Bar graph presenting the number of HeLa (J) and SiHa (L) clones. n = 5. versus control group or NC group, $^{**}P < 0.01$; versus shNUPR1 group, $^{\#\#}P < 0.01$; versus shTFE3 group, $^{\wedge\wedge}P < 0.01$.

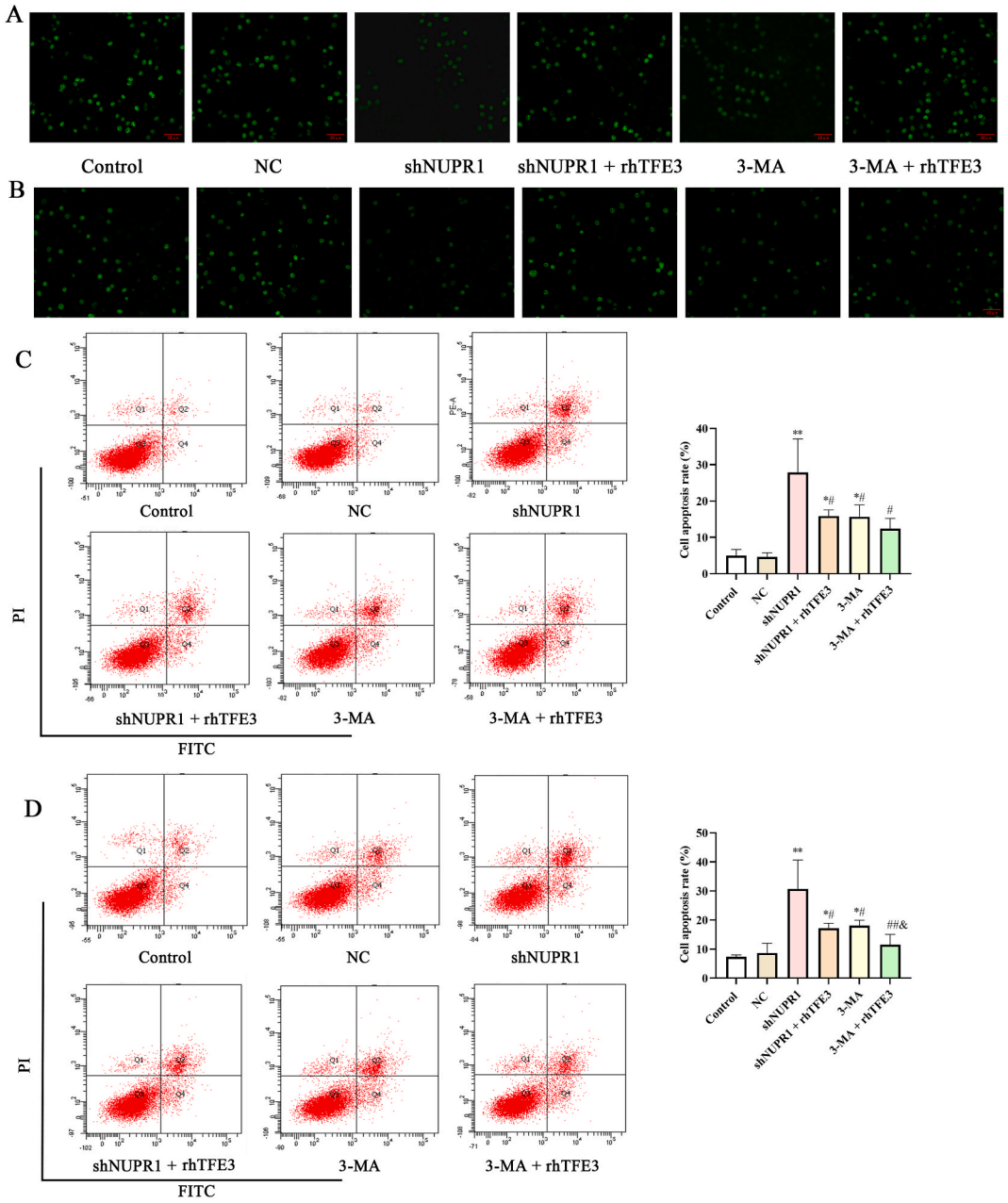

Fig. 4. Effect of NUPR1 knockdown on the proliferation and apoptosis of cervical cancer cells. Cells were divided into 6 groups, Control, NC (transfected with negative control shRNAs for NUPR1), shNUPR1, shNUPR1+rhTFE3, 3-MA, 3-MA + rhTFE3. EDU staining was used to observe the proliferation changes in HeLa (A) and SiHa (B) cells; The apoptosis in HeLa (C) and SiHa (D) cells were detect by flow cytometry. n = 3. versus control or NC group, *P < 0.05, **P < 0.01; versus shNUPR1 group, $^{\#}$P < 0.05, $^{\#\#}$P < 0.01; versus 3-MA group, $^{\&}$P < 0.05.

dislocation. The tumor weight was recorded, and tissues were collected for further study. Animal experiments were approved by Yantaishan Hospital (YSLZ2023053), and accordance with the approve guidelines.

2.12. Terminal deoxynucleotidyl transferase dUTP nick end labeling (TUNEL) assay

Tissues embedded in paraffin blocks were cut into 5 μm thick sections, dewaxed in xylene, and rehydrated with decreasing concentrations of ethanol. The TUNEL reaction solution (50 μL, Beyotime, Shanghai, China) was added, and incubated at 37 °C for 2 h in the dark condition. After the sections were washed twice with PBS, 3,3′- diaminobenzidine (DAB, Solarbio, Beijing, China) was added for color development, and the reaction was finally terminated with double distilled water. Hematoxylin (Solarbio) was used for

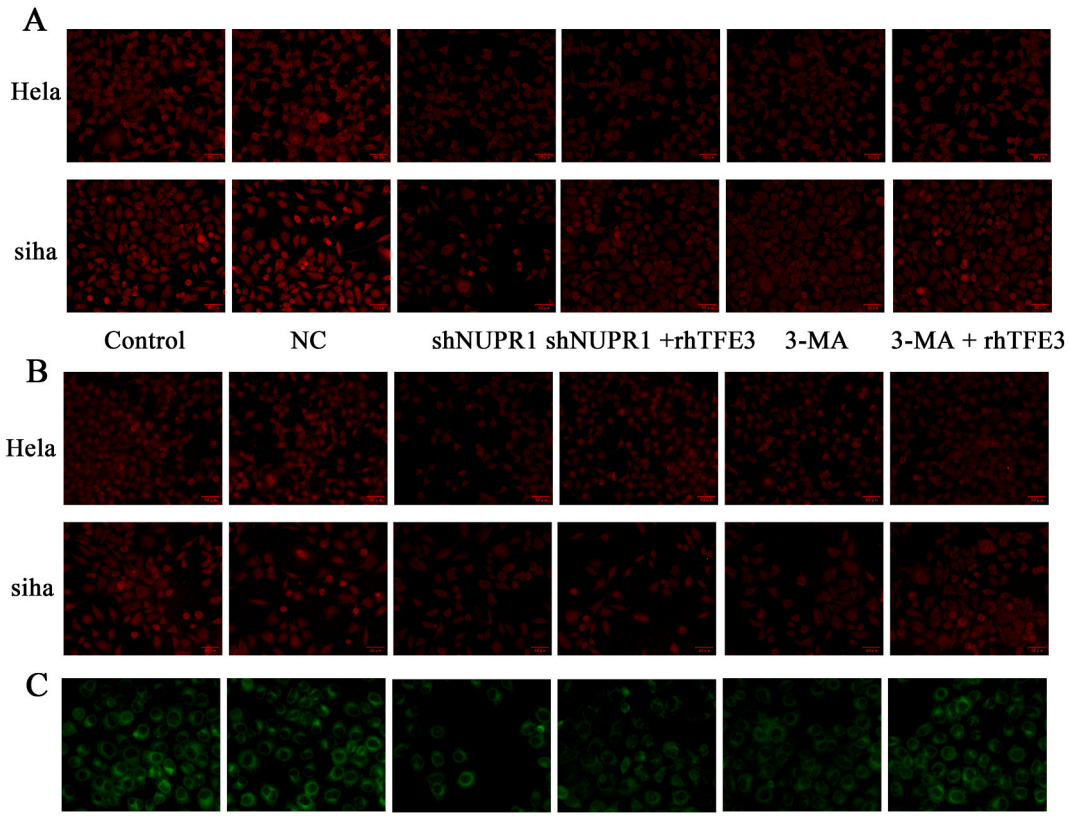

Fig. 5. Knockdown NUPR1 suppresses p62 and LC3B expression. Immunofluorescence detection of p62 expression in HeLa (A) and Siha (B) cells; Immunofluorescence detection of LC3B expression in HeLa (C) and SiHa (D) cells; E: LysoSensor Green DND-189 labeled HeLa cell lysosome changes. n = 3. (For interpretation of the references to color in this figure legend, the reader is referred to the Web version of this article.)

nuclear staining. To calculate the percentage of apoptotic cells, five non-repeating visual fields were randomly selected utlizing an optical microscope (Olympus, Japan).

2.13. Immunohistochemistry (IHC) staining

Tumor tissues were fixed in 4 % paraformaldehyde, embedded in paraffin, and cut into 4 μm thick slices. The slices were dewaxed with xylene, gradually hydrated with a gradient of 100–70 % ethanol, then washed with PBS. The slices were then treated with a sodium citrate buffer for heat-induced repair. The slices were treated with 30 % hydrogen peroxide solution for 10 min to block endogenous peroxidase activity. The slices were blocked with 5 % FBS at room temperature for 10 min after washing twice with PBS. Primary antibodies Ki67 (Beyotime, Shanghai, China), p62, LC3B, NUPR1, and TFE3 were incubated overnight at 4 °C, then washed thrice with PBS. The slices were then incubated with a specific biotinylated secondary antibody (Bioss, Beijing China) at 37 °C for 60 min, and then re-stained with DAB and hematoxylin. Under an optical microscope (Olympus, Tokyo, Japan), the stained sections were photographed.

2.14. Western blotting

Cells or tissues were collected, centrifuged at 4 °C, 12,000×*g* for 5 min. Each sample was subjected to separation of 50 μg of protein using 8 % SDS-PAGE, followed by transfer onto a PVDF membrane. The membranes were then treated with 5 % skim milk for 2 h at room temperature and incubated overnight with the primary antibody at 4 °C. After washing thrice with TBST, the membrane was incubated with the corresponding horseradish peroxidase-conjugated secondary antibody (Bioybrt, UK) for 1 h at room temperature. The visualization of bands and calculation of relative protein expression were performed using an enhanced chemiluminescence reagent (Beyotime, Shanghai, China) and ImageJ software (NIH, USA).

2.15. Statistical analysis

The study employed Spearman's correlation analysis to ascertain the correlation between NUPR1 and TFE3 expression. Kaplan-Meier curves were generated and p-values and hazard ratios (HR) with 95 % confidence intervals (CI) were calculated using log-

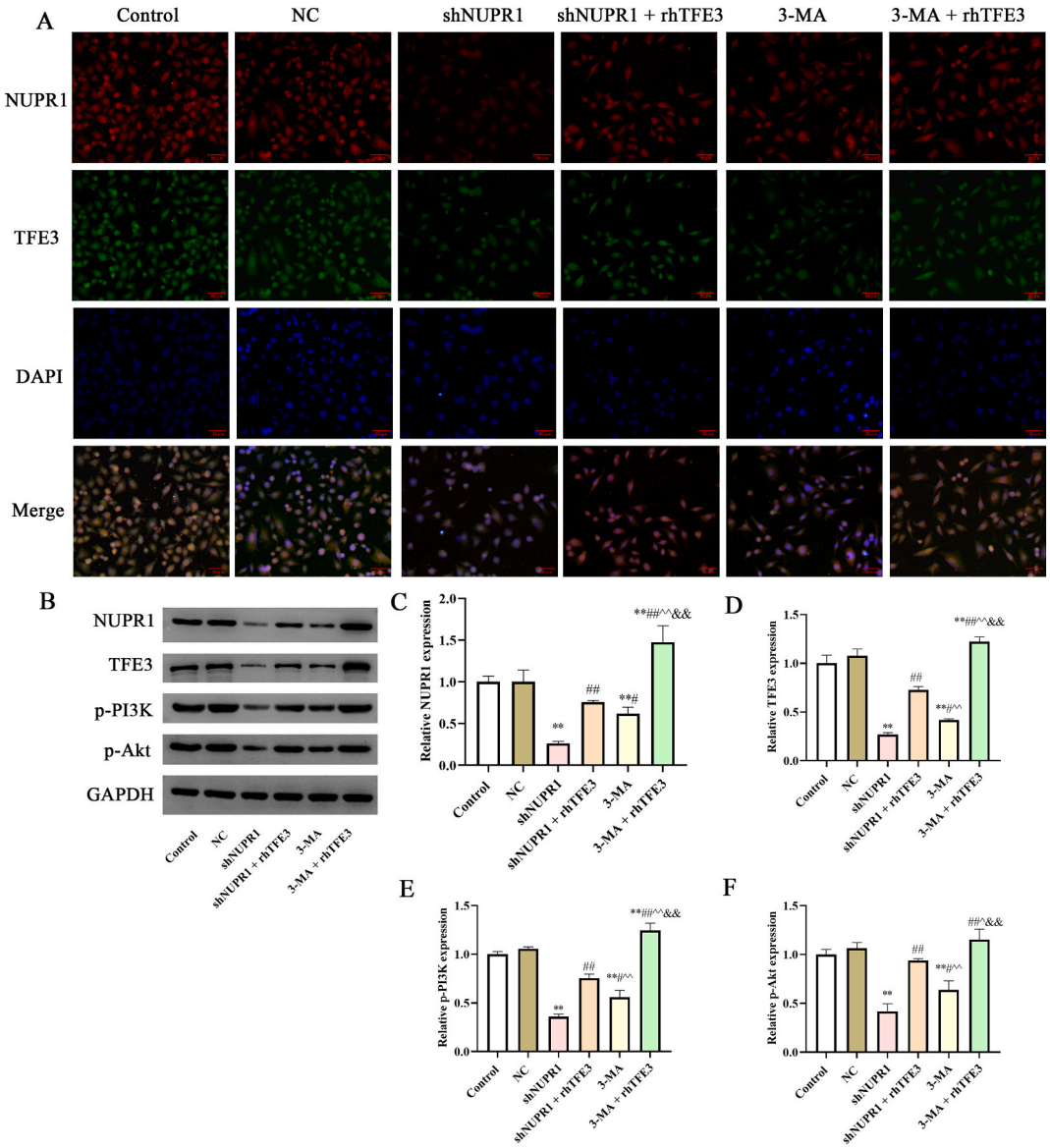

Fig. 6. NUPR1 knockdown inhibits the p-PI3K and p-Akt expression. A: Immunofluorescence detection of NUPR1 and TFE3 co-localization in HeLa cells; B: Western blot analysis was used to detect NUPR1, TFE3, p-PI3K, and p-Akt expression in HeLa cells; Bar graphs represent the quantification of protein expression levels of NUPR1 (C), TFE3 (D), p-PI3K (E), and p-Akt (F). n = 3. versus control or NC group, *P < 0.05, **P < 0.01; versus shNUPR1 group, $^{\#}$P < 0.05, $^{\#\#}$P < 0.01; versus shNUPR1 + rhTFE3 group, $\hat{}$P<0.05, $\hat{}\hat{}$P<0.01; versus 3-MA group, $^{\&}$P < 0.05, $^{\&\&}$P < 0.01.

rank tests and univariate Cox proportional hazards regression. The analysis methods and R packages were implemented using R (Foundation for Statistical Computing 2020) version 4.0.3. Intergroup comparisons were conducted using analysis of variance (ANOVA) followed by Tukey's post-hoc analysis. Statistical significance was established at P < 0.05.

3. Results

3.1. NUPR1 and TFE3 are highly expressed in cervical cancer and are associated with poor prognosis in patients

The present study utilized the TCGA online database to investigate the association between NUPR1 and TFE3 expression levels in cervical cancer. The findings, as depicted in Fig. 1A, revealed a positive correlation between NUPR1 and TFE3 mRNA levels in cervical cancer. Furthermore, the study explored the prognostic significance of NUPR1 and TFE3 in cervical cancer, with the results indicating a hazard ratio (HR) > 1, suggesting that NUPR1 and TFE3 are potential risk factors for cervical cancer. Notably, high expression levels of

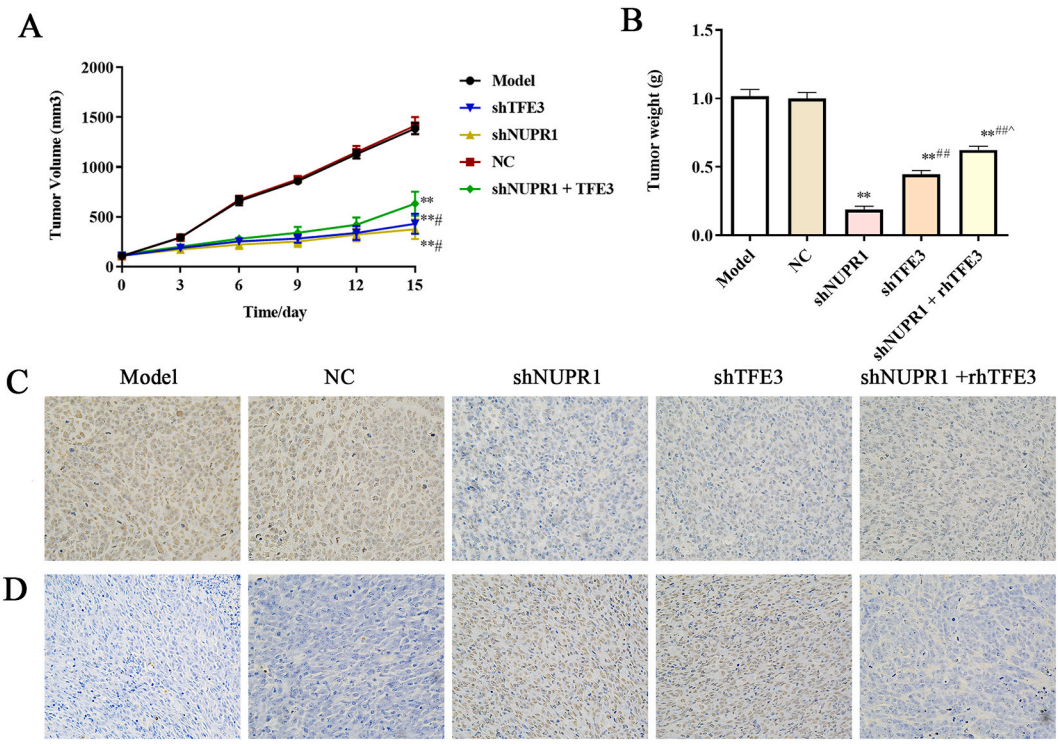

Fig. 7. NUPR1 knockdown suppressed the tumor growth and promoted cell apoptosis *in vivo*. A: Volume changes of transplanted tumors in nude mice; B: Changes in the weight of tumors transplanted in nude mice; C: Immunohistochemical detection of changes in tumor tissues, Ki67; D: TUNEL was used to detect apoptosis in tumor tissues. n = 6. versus model or NC group, *P < 0.05, **P < 0.01; versus shNUPR1 group, $^{\#}$P < 0.05, $^{\#\#}$P < 0.01; versus shTFE3 group, $\hat{}$P < 0.05.

NUPR1 and TFE3 were found to be associated with poor patient prognosis (Fig. 1B). The ROC curve analysis demonstrated that the highest AUC value for one year was 0.665, indicating that high NUPR1 and TFE3 expression levels may serve as a predictive biomarker for cervical cancer prognosis (Fig. 1C).

3.2. Knockdown of NUPR1 or TFE3 suppresses the migration, invasion, and proliferation of cervical cancer cells

To verify the roles of NUPR1 and TFE3 in cervical cancer, shRNAs were used to inhibit NUPR1 and TFE3 expression. The results are shown in Fig. 2A–D, where shRNA significantly suppressed NUPR1 and TFE3 expression in cervical cancer cells (P < 0.01).

To assess the effects of NUPR1 or TFE3 knockdown on cell migration, invasion, and proliferation, we conducted scratch migration, Matrigel Transwell invasion, and clone formation experiments. NUPR1 and TFE3 knockdown decreased cell migration, invasion, and proliferation. Importantly, when shNUPR1 was combined with rhTFE3, cell migration, invasion, and proliferation were partially increased (P < 0.01, Fig. 3A-L).

3.3. NUPR1 knockdown weakens the effect of TFE3 and autophagy inhibition on NUPR1 and TFE3 expression and cell apoptosis

3-MA is a common autophagy inhibitor [19]. Our data show that the number of EdU-positive cells were decreased after 3-MA treatment (Fig. 4A and B). Flow cytometric analysis of apoptosis showed that NUPR1 knockdown significantly increased the rate of apoptosis in cervical cancer cells. After co-treatment with shNUPR1 and rhTFE3, the apoptotic rate was decreased (P < 0.01). Further, 3-MA treatment also increased the apoptotic rate of the cells. However, the apoptotic rate of the cells decreased after cotreatment with 3-MA and rhTFE3 (Fig. 4C, D, P < 0.05). These results indicated that NUPR1 knockdown could promote apoptosis in cervical cancer cells.

3.4. NUPR1 knockdown affected autophagy-related proteins expression

Immunofluorescence results showed that NUPR1 knockdown significantly suppressed the expression of the autophagy-related proteins, p62 and LC3B, and that rhTFE3 treatment partially reversed the effect of NUPR1 knockdown. 3-MA inhibited p62 and LC3B expression. Further, rhTFE3 treatment reversed the inhibitory effects of 3-MA (Fig. 5A and B). NUPR1 knockdown significantly reduced the number of lysosomes in HeLa cells and rhTFE3 treatment partially reversed this effect of NUPR1 knockdown (Fig. 5C).

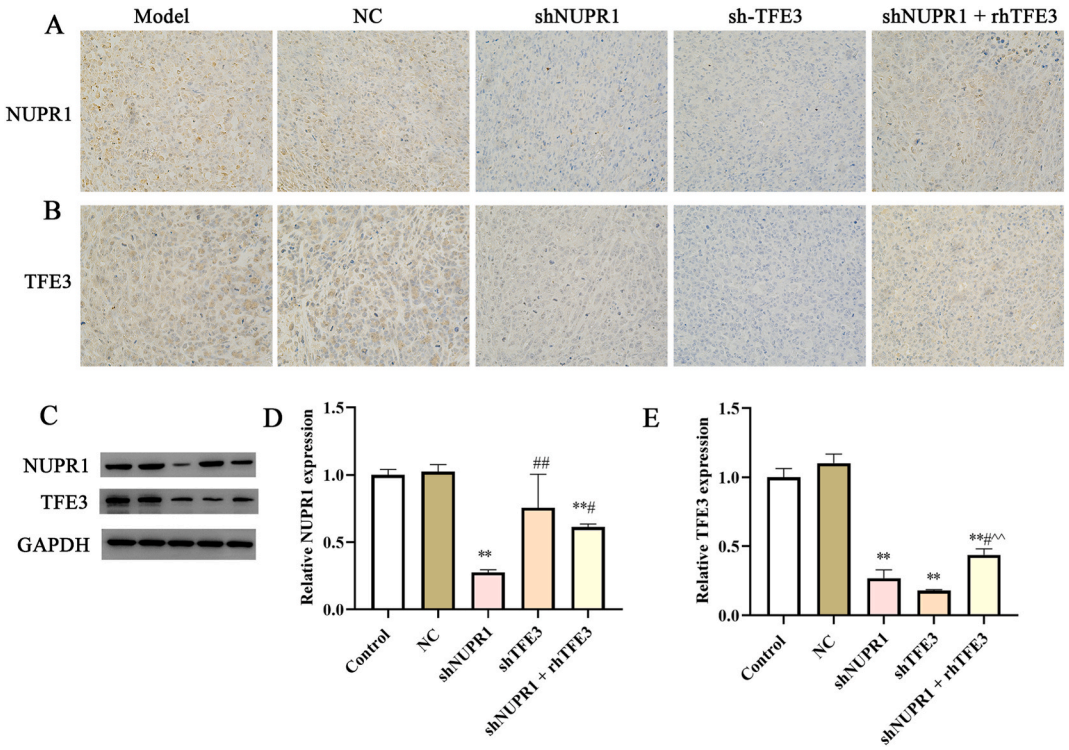

Fig. 8. NUPR1 and TFE3 expression in tumor tissues. Immunohistochemical staining was utilized to detect the NUPR1 (A) and TFE3 (B) positive expression in tumor tissues; n = 6. C: Western blot was utilized to detect the expression of NUPR1 and TFE3 in tumor tissues; Bar graphs represent the quantification of NUPR1 (D) and TFE3 (E) protein expression levels. n = 3. versus model or NC group, *P < 0.05, **P < 0.01; versus shNUPR1 group, $^{\#}$P < 0.05, $^{\#\#}$P < 0.01; versus shTFE3 group, $^{\wedge\wedge}$P < 0.01.

3.5. NUPR1 knockdown blocks the PI3K/Akt pathway

We examined the activity of the PI3K/Akt pathway in cervical cancer cells after NUPR1 knockdown. As expected, NUPR1 and TFE3 expression decreased after NUPR1 knockdown. Further. 3-MA treatment also inhibits the expression of NUPR1 and TFE3 Additionally, treatment with rhTFE3 partially reversed the effects of NUPR1 knockdown and 3-MA treatment. Furthermore, we detected the phosphorylation of PI3K and Akt, and the results showed that NUPR1 knockdown and 3-MA treatment both reduced the levels of p-PI3K and p-Akt (Fig. 6A–F, P < 0.05). Further, rhTFE3 treatment reversed the suppressed effects of NUPR1 knockdown and 3-MA treatment on p- PI3K, and p-Akt expression (P < 0.05).

3.6. The inhibitory effect of NUPR1 knockdown on the growth of tumors transplanted in vivo

NUPR1 and TFE3 knockdown inhibited the growth of transplanted tumors (Fig. 7A and B, P < 0.01). IHC staining showed that NUPR1 and TFE3 knockdown could reduce the positive expression of Ki67 (Fig. 7C). TUNEL staining revealed that NUPR1 and TFE3 knockdown promoted tumor cell apoptosis. Further, rhTFE3 treatment partially reversed the inhibitory influence of NUPR1 knockdown on tumor growth (Fig. 7D).

3.7. NUPR1 and TFE3 expression in tumor tissue

The expression level of NUPR1 was substantially reduced after NUPR1 knockdown, and that the expression of TFE3 was reduced compared to that in the model and NC groups (P < 0.05). Similarly, after TFE3 knockdown, TFE3 expression level was substantially reduced, and that of NUPR1 was also significantly reduced (Fig. 8A–E, P < 0.05). However, rhTFE3 treatment partially reversed the suppressed effects of NUPR1 knockdown.

3.8. NUPR1 knockdown could suppress autophagy-related proteins and PI3K/Akt expression in vivo

IHC staining showed that NUPR1 or TFE3 knockdown significantly inhibited p62 and LC3B expression. Further analysis showed that the knockdown of NUPR1 and TFE3 suppressed the levels of lamp1, lamp2, p-PI3K, and p-Akt. Further, rhTFE3 treatment partially reversed the effect of NUPR1 knockdown on the levels of p62, LC3B, lamp1, lamp2, p-PI3K, and p-Akt (Fig. 9A–G, P < 0.05).

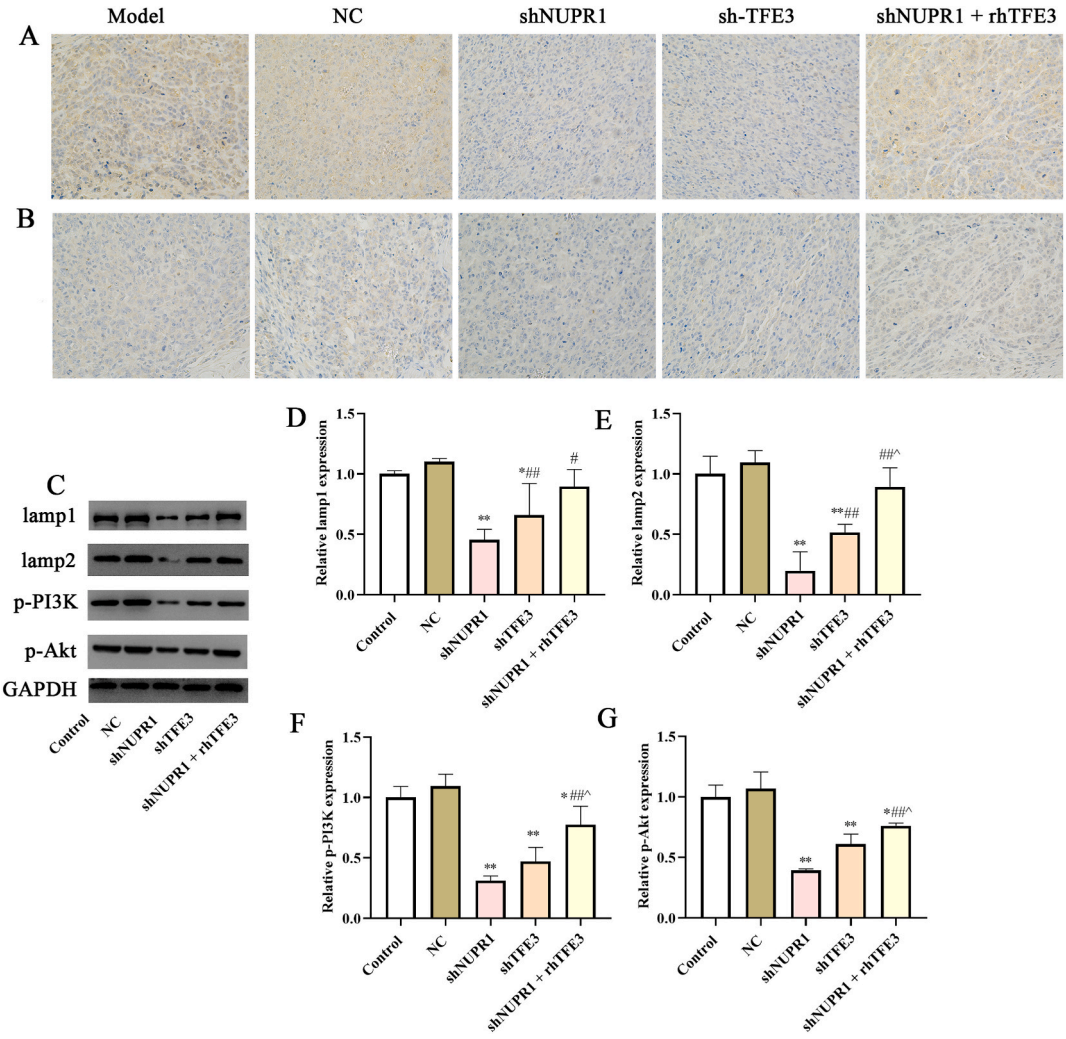

Fig. 9. NUPR1 knockdown suppressed autophagy-related proteins and PI3K/Akt signaling expression. Immunohistochemical staining was utilized to detect the expression of p62 (A) and LC3B (B) in tumor tissues; n = 6. C: Western blot analysis was utilized to detect lamp1, lamp2, p-PI3K, and p-Akt expression levels; Bar graphs present the quantification of lamp1 (D), lamp2 (E), p-PI3K (F), and p-Akt (G) levels. n = 3. versus model or NC group, *P < 0.05, **P < 0.01; versus shNUPR1 group, $^{\#}$P < 0.05, $^{\#\#}$P < 0.01; versus shTFE3 group, $^{\wedge}$P < 0.05.

4. Discussion

Cervical cancer is characterized by high rates of metastasis, recurrence, and mortality. Owing to the lack of effective treatment strategies, cervical cancer poses a significant threat to human health. To develop effective therapeutic drugs, identifying molecules that control the recurrence and metastasis of cervical cancer is essential. In the current study, we used TCGA data to demonstrate a positive correlation between NUPR1 and TFE3 expression in cervical cancer and their association with short-term adverse prognosis. These analyses provide new insights into NUPR1-TFE3 as a potential therapeutic target against cervical cancer progression.

Studies have confirmed that NUPR1 promotes metastasis and chemotherapy resistance in prostate, liver, breast, and ovarian cancers [4,8,10,20]. Previous studies have also confirmed that NUPR1 promotes epithelial mesenchymal transformation and cell proliferation in oral squamous cell carcinoma [21,22]. Recent studies indicate that NUPR1 promotes the development of breast cancer and oral squamous cell carcinoma by inducing autophagy via TFE3 [13,23]. Our results show that NUPR1 and TFE3 knockdown reduced the migration, invasion, and proliferation of cervical cancer cells. NUPR1 knockdown was more effective than 3-MA knockdown at inhibiting cervical cancer cell proliferation and promoting apoptosis. Interestingly, rhTFE3 partially reverses the effect of NUPR1 knockdown. Similarly, rhTFE3 partially reverses the inhibitory effects of 3-MA. This result can be explained by the fact that the effect of NUPR1 is related to TFE3 activity.

Under hypoxic and hunger conditions, autophagy provides cancer cells with a means of survival. NUPR1 is the main transcription factor regulating autophagy. Recent studies have shown that NUPR1 knockout blocks autophagic flux in cancer cells and increases apoptosis in liver cancer cells [24]. NUPRl knockout leads to premature aging of breast cancer cells by damaging the autolytic process

[10]. Further, the autophagic flow maintained by NUPR 1 is essential for lung cancer development [25]. In this study, we found that NUPR1 knockdown disrupted lysosomal function and inhibited the expression of LC3B, an autophagy marker, as well as p62. Further, NUPR1 knockdown also inhibited the expression of lamp1 and lamp2. These results indicate that the inhibitory effect of NUPR1 knockdown on cervical cancer was related to cell inhibition. TFE3 is a key regulator of gene expression related to the formation and degradation of autophagosomes and autolysosomes. Research has shown that TFE3-dependent autophagic lysosomal activation is essential for lysosomal function [26]. Interestingly, our data showed that after NUPR1 knockdown, the expression of TFE3 was significantly reduced, and that TFE3 overexpression reversed the inhibition of lysosomal function induced by NUPR1 knockdown in cervical cancer cells. Our results thus indicate a connection between NUPR1and TFE3 in cervical cancer.

In various tumors, the PI3K/Akt signaling pathway is abnormally activated, resulting in drug resistance [27–29]. In cervical cancer, the PI3K/Akt signaling pathway is dysregulated, and its activation can promote cancer cell proliferation and affect cancer cell sensitivity to cisplatin drugs [30,31]. Our results showed that the activity of the PI3K/Akt signaling pathway was suppressed after NUPR1 knockdown, and that TFE3 overexpression reversed the inhibitory effect of NUPR1 knockdown. Thus, these results suggest that the downstream mechanism of the NUPR1 knockout may be related to the PI3K/Akt signaling pathway.

5. Conclusion

Taken together, our results indicate that the NUPR1-TFE3 axis mediated PI3K/Akt pathway contributes to cervical cancer development, and that the NUPR1-TFE3 axis can be used for preventing and treating cervical cancer. Thus, our study provides new targets for cervical cancer treatment.

Funding

This study was financially supported by the Yantai Science and Technology Innovation Development Plan (2021YD041).

Data availability statement

Data will be made available on request.

CRediT authorship contribution statement

Xiaoguang Wang: Writing - review & editing, Writing - original draft, Funding acquisition, Formal analysis, Data curation, Conceptualization. **Ke Wang:** Writing - review & editing, Writing - original draft, Visualization, Formal analysis, Data curation, Conceptualization. **Xiuli Wang:** Writing - review & editing, Writing - original draft, Data curation, Conceptualization.

Declaration of competing interest

The authors declare that they have no known competing financial interests or personal relationships that could have appeared to influence the work reported in this paper.

References

[1] X. Yang, et al., Prognostic nomograms predicting survival in patients with locally advanced cervical squamous cell carcinoma: the first nomogram compared with revised FIGO 2018 staging system, Front. Oncol. 10 (2020) 591700.
[2] W.Y. Wang, et al., Delivery of folic acid-modified liposomal curcumin for targeted cervical carcinoma therapy, Drug Des. Dev. Ther. 13 (2019) 2205–2213.
[3] L. Peirson, et al., Screening for cervical cancer: a systematic review and meta-analysis, Syst. Rev. 2 (2013) 35.
[4] P. Santofimia-Castaño, et al., Targeting the stress-induced protein NUPR1 to treat pancreatic adenocarcinoma, Cells 8 (11) (2019).
[5] R. Zhou, et al., Nupr1 mediates renal fibrosis via activating fibroblast and promoting epithelial-mesenchymal transition, Faseb. J. 35 (3) (2021) e21381.
[6] X. Xiong, et al., Pancreatic islet-specific overexpression of Reg3β protein induced the expression of pro-islet genes and protected the mice against streptozotocin-induced diabetes mellitus, Am. J. Physiol. Endocrinol. Metab. 300 (4) (2011) E669–E680.
[7] D. Taïeb, et al., Inactivation of stress protein p8 increases murine carbon tetrachloride hepatotoxicity via preserved CYP2E1 activity, Hepatology 42 (1) (2005) 176–182.
[8] Y. Zhan, et al., NUPR1 contributes to radiation resistance by maintaining ROS homeostasis via AhR/CYP signal axis in hepatocellular carcinoma, BMC Med. 20 (1) (2022) 365.
[9] W. Huo, et al., Epigenetic silencing of microRNA-874-3p implicates in erectile dysfunction in diabetic rats by activating the Nupr1/Chop-mediated pathway, Faseb. J. 34 (1) (2020) 1695–1709.
[10] L. Wang, et al., Transcriptional coregualtor NUPR1 maintains tamoxifen resistance in breast cancer cells, Cell Death Dis. 12 (2) (2021) 149.
[11] A. Li, et al., NUPR1 silencing induces autophagy-mediated apoptosis in multiple myeloma cells through the PI3K/AKT/mTOR pathway, DNA Cell Biol. 39 (3) (2020) 368–378.
[12] N.E. Real, et al., Molecular markers of DNA damage and repair in cervical cancer patients treated with cisplatin neoadjuvant chemotherapy: an exploratory study, Cell Stress Chaperones 22 (6) (2017) 811–822.
[13] H. Xiao, et al., NUPR1 promotes the proliferation and migration of breast cancer cells by activating TFE3 transcription to induce autophagy, Exp. Cell Res. 418 (1) (2022) 113234.
[14] J.A. Martina, et al., The nutrient-responsive transcription factor TFE3 promotes autophagy, lysosomal biogenesis, and clearance of cellular debris, Sci. Signal. 7 (309) (2014) ra9.
[15] M. Palmieri, et al., Characterization of the CLEAR network reveals an integrated control of cellular clearance pathways, Hum. Mol. Genet. 20 (19) (2011) 3852–3866.
[16] C. Settembre, et al., TFEB controls cellular lipid metabolism through a starvation-induced autoregulatory loop, Nat. Cell Biol. 15 (6) (2013) 647–658.

[17] C. Settembre, et al., TFEB links autophagy to lysosomal biogenesis, Science 332 (6036) (2011) 1429–1433.
[18] N. Pastore, et al., TFE3 regulates whole-body energy metabolism in cooperation with TFEB, EMBO Mol. Med. 9 (5) (2017) 605–621.
[19] T. Khan, et al., Autophagy modulators for the treatment of oral and esophageal squamous cell carcinomas, Med. Res. Rev. 40 (3) (2020) 1002–1060.
[20] J. Yu, et al., Oncogenic role of NUPR1 in ovarian cancer, OncoTargets Ther. 13 (2020) 12289–12300.
[21] W. Jiang, et al., CircRNA HIPK3 promotes the progression of oral squamous cell carcinoma through upregulation of the NUPR1/PI3K/AKT pathway by sponging miR-637, Ann. Transl. Med. 9 (10) (2021) 860.
[22] W. Huang, J. Cao, X. Peng, LINC01234 facilitates growth and invasiveness of oral squamous cell carcinoma through regulating the miR-637/NUPR1 axis, Biomed. Pharmacother. 120 (2019) 109507.
[23] T. Fan, et al., NUPR1 promotes the proliferation and metastasis of oral squamous cell carcinoma cells by activating TFE3-dependent autophagy, Signal Transduct. Targeted Ther. 7 (1) (2022) 130.
[24] G. Augello, et al., The NUPR1/p73 axis contributes to sorafenib resistance in hepatocellular carcinoma, Cancer Lett. 519 (2021) 250–262.
[25] Y. Mu, et al., NUPR1 maintains autolysosomal efflux by activating SNAP25 transcription in cancer cells, Autophagy 14 (4) (2018) 654–670.
[26] R.M. Perera, C. Di Malta, A. Ballabio, MiT/TFE family of transcription factors, lysosomes, and cancer, Annu. Rev. Cell Biol. 3 (2019) 203–222.
[27] A. Guerrero-Zotano, I.A. Mayer, C.L. Arteaga, PI3K/AKT/mTOR: role in breast cancer progression, drug resistance, and treatment, Cancer Metastasis Rev. 35 (4) (2016) 515–524.
[28] F. Liang, et al., The crosstalk between STAT3 and p53/RAS signaling controls cancer cell metastasis and cisplatin resistance via the Slug/MAPK/PI3K/AKT-mediated regulation of EMT and autophagy, Oncogenesis 8 (10) (2019) 59.
[29] N. Koundouros, G. Poulogiannis, Phosphoinositide 3-kinase/akt signaling and redox metabolism in cancer, Front. Oncol. 8 (2018) 160.
[30] X. Chen, et al., SPP1 inhibition improves the cisplatin chemo-sensitivity of cervical cancer cell lines, Cancer Chemother. Pharmacol. 83 (4) (2019) 603–613.
[31] X.R. Shu, et al., PAK4 confers the malignance of cervical cancers and contributes to the cisplatin-resistance in cervical cancer cells via PI3K/AKT pathway, Diagn. Pathol. 10 (2015) 177.